ELSEVIER

Soil Dynamics and Earthquake Engineering 22 (2002) 719–731

SOIL DYNAMICS AND EARTHQUAKE ENGINEERING

www.elsevier.com/locate/soildyn

Evaluation of models for Fourier amplitude spectra for the Taiwan region

Vladimir Sokolov[a,b,*], Chin-Hsiung Loh[b], Kuo-Liang Wen[c]

[a]*Geophysical Institute, Karlsruhe University, Hertzstr. 16, 76187 Karlsruhe, Germany*
[b]*National Center for Research on Earthquake Engineering, 200, Sec. 3, Hsinhai Road, Taipei, Taiwan, ROC*
[c]*Institute of Applied Geology, National Central University, 38, Wu-chuan Li, Chung-li, Taiwan, ROC*

Accepted 30 March 2002

Abstract

In the Taiwan region, the empirical spectral models for estimating ground-motion parameters were obtained recently on the basis of recordings of small to moderate ($5.0 \leq M_L \leq 6.5$) earthquakes. A large collection of acceleration records from the $M_L = 7.3$ Chi-Chi earthquake (21 September, 1999) makes it possible to test the applicability of the established relationships in the case of larger events. The comparison of ground-motion parameters (Fourier amplitude spectra, peak accelerations and response spectra), which were calculated using the models, and the observed data demonstrates that the models could provide an accurate prediction for the case of the Chi-Chi earthquake and the largest aftershocks. However, there are some peculiarities in the ground-motion frequency content and attenuation that, most probably, are caused by the features of the rupture process of the large shallow earthquake source.

Keywords: Acceleration spectra; Scaling law; Attenuation relation

1. Introduction

Procedures of seismic hazard assessment are based on ground-motion attenuation relationships, which can be derived from statistical analyses of recorded ground motions or, in conditions of limited strong-motion records, can be obtained from the available literature sources. Ideally, these attenuation models should consider regional earthquake source and propagation path effects and local site response peculiarities. However, the empirical databases usually consist on the recording, which were obtained during the events of small and moderate magnitudes. Therefore, a question is arising—'is it possible to use these relationships in the case of larger events'? The lack of strong motion data for large earthquakes results in using of several seismological models. An important criterion for any simulation procedure is its validation against recorded ground motion. Every strong earthquake provides a unique opportunity both to verify the accepted attenuation models, and to update empirical relationships.

In recent years, Fourier amplitude spectrum is widely used for prediction of ground-motion parameters [5,7,8,9,11,20] on the basis of stochastic approach [10]. The frequency content of seismic ground motion was studied in different seismic regions and the various model and relations between the level of the Fourier-acceleration spectra, earthquake magnitude and distance have been proposed. Several models are based on statistical analysis of empirical data to estimate an equation of regression [3,6,14,28,35]. A large number of frequency-dependent regression coefficient are determined when using this approach. The information on the local site condition should be known, otherwise this regression will describe so-called 'average soil'. In the other models, the spectrum is represented by analytical expressions describing source, propagation, and site effect, separately [4,9,11,16,18,25,27,29–31,36]. Parameters of the expressions can be determined on the basis of empirical data, and it is not necessary to know detailed information on local site conditions. These models (very simple or complicated) revealed some common features reflecting the source mechanism and travel-path influence, however different regional and local conditions may produce significant differences in spectral contents of the ground-motion records. In the Taiwan region, the empirical spectral models for estimating ground-motion parameters were obtained recently on the basis of recordings of small to moderate ($5.0 \leq M_L \leq 6.5$) earthquakes [31]. A large collection of

* Corresponding author. Address: National Center for Research on Earthquake Engineering, 200, Sec. 3, Hsinhai Road, Taipei, Taiwan, ROC. Tel./fax: +886-2-2732-2223.
E-mail address: vladimir.sokolov@gpi.uni-karlsruhe.de (V. Sokolov).

0267-7261/02/$ - see front matter
PII: S0267-7261(02)00026-X

acceleration records from the recent $M_L = 7.3$ Chi-Chi earthquake and its large ($M_L > 6.5$) aftershocks (more than 1000 records obtained at distances up to 120–140 km) [24,26,37] allows us to test the applicability of the established relationships in the case of large shallow thrust earthquakes.

In this paper, we compare the ground-motion parameters (Fourier amplitude spectra, peak accelerations and response spectra) which were estimated for different soil conditions (hard rock and average soil) using the models, and the data observed during the Chi-Chi earthquake. The comparison makes it possible to conclude that the recently established regional empirical models for Fourier amplitude spectra, which are used for calculation of PGA and response spectra by stochastic approach, allow satisfactory prediction of ground-motion parameters for large earthquakes. However, the models should be revised to satisfy the peculiarities of ground-motion excitation and propagation during shallow earthquakes in the Taiwan region.

2. Empirical spectral models for the Taiwan region

The empirical models (Fourier amplitude spectra of ground acceleration) for estimating design input ground-motion parameters in the Taiwan region have been obtained before the Chi-Chi earthquake on the basis of the recordings (1380 accelerograms) of small and moderate earthquakes ($4.5 < M_L < 6.6$) [30,31]. The general model of radiated spectra, describing the Fourier acceleration spectrum A at frequency f, was considered in the following way [10]

$$A(f) = (2\pi f)^2 CS(f)D(R,f)I(f) \quad (1)$$

where C is the scaling factor; $S(f)$ is the source spectrum; $D(R,f)$ is the attenuation function, and $I(f)$ represents frequency-dependent site response. The scaling factor is given by

$$C = (\langle R_{\theta\phi}\rangle FV)/(4\pi\rho V_S^3 R^b) \quad (2)$$

where $\langle R_{\theta\rho}\rangle$ is the radiation coefficient, F is the free surface amplification, V represents the partitions of the vector into horizontal components, ρ and V_S are the density and shear velocity in the source region, and R is the hypocentral distance. A commonly used source function $S(f)$ in the Brune's model [13] is

$$S(f) = M_0/[1 + (f/f_0)^2] \quad (3)$$

For the Brune's model, the source acceleration spectrum at low-frequencies increases as f^2 and approaches a value determined by f_0 (corner frequency) and M_0 at frequencies $f > f_0$. The value of f_0 can be found from the relation $f_0 = 4.9 \times 10^6 V_S(\Delta\sigma/M_0)^{1/3}$. Here $\Delta\sigma$ is the stress parameter in bars, M_0 is the seismic moment in dyn cm and V_S in km/s. The level of the spectrum remains approximately constant for frequencies above f_0 until the cut-off frequency f_{max} is approached. The amplitude of the spectrum decays rapidly at frequencies above f_{max}. The function $D(R,f)$ accounts for frequency-dependent attenuation that modifies the spectral shape. It depends on the hypocentral distance (R), regional crustal material properties, the frequency-dependent regional quality factor Q, and f_{max}. These effects are represented by the equation

$$D(R,f) = \exp[-\pi f R/Q(f)V_S]P(f,f_{max}) \quad (4)$$

where $P(f,f_{max})$ is a high-cut filter [2]

$$P(f) = \exp(-\pi\kappa f) \quad (5)$$

The results of our previous study reveal that the acceleration spectra of most significant part of the records, starting from S-wave arrival, for hypothetical very hard rock (VHR) sites ($r = 2.8$ g/cm^3, $V_S = 3.8$ km/s, $I(f) = 1$) in the Taiwan region can be modelled accurately by the single-corner frequency Brune ω^{-2} source model with the magnitude-dependent stress parameter $\Delta\sigma$, that should be determined using recently proposed regional relationships between seismic moment (M_0) and magnitude (M_L) [22]

$$\log_{10} M_0 = (19.043 \pm 0.533) + (0.914 \pm 0.035)M_L \quad (6)$$

and between $\Delta\sigma$ and M_0 [36]

$$\log 10\ \Delta\sigma = -3.3976 + 0.2292 \log_{10} M_0 \pm 0.6177 \quad (7)$$

In Ref. [36] it has been noted that the $\Delta\sigma$ values estimated using his relationships should be treated as upper-boundary values. Frequency-dependent attenuation of spectral amplitudes with distance may be described using quality factor $Q = 225f^{1.1}$ for deep (hypocentral depth more than 35 km) earthquakes and $Q = 125f^{0.8}$ for shallow earthquakes, and a kappa filter ($k = 0.03$–0.04) may be used to modify the spectral shape. When considering geometrical spreading in the form $1/R^b$ (Eq. (2)), attenuation of the direct waves is described using $b = 1.0$ for $R_1 < 50$ km; for transition zone where the direct wave is joined by postcritical reflections from mid-crustal interfaces and the Moho-discontinuity ($50 < R_2 < 150$–170 km) $b = 0.0$,and attenuation of multiply reflected and refracted S-waves is described by $b = 0.5$ for $R_3 > 170$ km.

Two spectral models were developed for the Taiwan region [31], namely: the model 1—the earlier mentioned ω-square model for VHR site (Fig. 1), and the model 2—empirical spectra estimated for reference distance $R = 1$ km (Fig. 2(a), solid lines). These spectra, averaging the variety of site conditions from rock to soft soil of different thickness, correspond to the so-called average soil condition, and they were estimated for magnitude ranges $5.0 < M_L < 5.5$; $5.5 < M_L < 6.0$, and $6.0 < M_L < 6.5$. In order to extend the model 2 for the larger magnitudes, the logarithmic increments (β_M) of spectral amplitudes (A) per unit of magnitude were calculated for considered frequencies (0.2–12 Hz) in the following form $\beta_M(f) = \Delta \log A(f)/\Delta M$, where ΔM is the increment of magnitude, and $A(f)$ is the 'reference distance' spectral amplitudes (mean values, Fig. 2(a)). Fig. 2(b) shows the values β_M

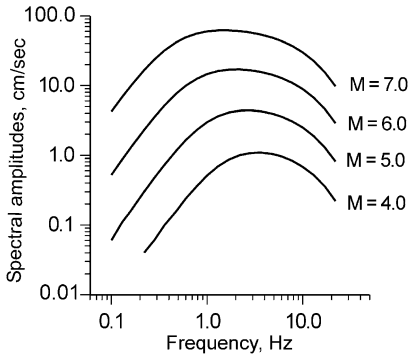

Fig. 1. VHR theoretical ω-square spectra of ground acceleration for the Taiwan region, distance $R = 10$ km.

which were calculated for the earlier mentioned magnitude ranges, and the averaged values which were used for estimation of spectral amplitudes for the larger magnitudes (Fig. 2(b), dashed lines). The relation $\beta_M(f)$ shows that the values of β_M increase with decreasing of frequency and they are nearly constant in low-frequency range. By the other words, as the source energy increases, the intensity of low-frequency vibrations increases more rapidly than that of high-frequency vibrations. The fact agrees with the results of the previous studies of the β_M coefficients [14,28]. When using the model 2, the average soil spectrum at a distance R was calculated by multiplication of the reference distance spectrum by $R^b \exp(-\pi f R/Q(f)V_S)$, where factor $Q = 225f^{1.1}$ for deep (depth more than 35 km) earthquakes and $Q = 125f^{0.8}$ for shallow earthquakes.

It is assumed that the same attenuation relationship ($Q = Q_0 f^n$) could be applied for the both developed spectral models (average soil and VHR), therefore the spectrum, representing ground acceleration for VHR (S_{VHR}), should fit the mean values of average soil spectrum (S_{AS}) at low-frequencies ($f < 0.1$–0.2 Hz), and it should generally be less than the average soil spectrum at higher frequencies. The ratio between these spectra S_{AS}/S_{VHR} may be considered as the spectral amplification for average soil. Let us suppose that the amplitudes of site amplification do not depend on the ground-motion intensity (linear amplification). The requirement could be accepted for magnitudes $M < 6.5$. If the spectral ratios for various magnitudes do not differ significantly, i.e. empirical average soil spectra may be obtained by multiplication of theoretical VHR spectra by the same amplification function, therefore it is possible to conclude that the VHR model describes the dependence between spectral amplitudes and earthquake parameters with sufficient accuracy.

Fig. 3(a) shows an example of comparison between ground acceleration spectra evaluated using these two models (VHR spectrum, $M_L = 6.3$; average soil spectrum, $6.0 < M_L < 6.5$) for distance 20 km. When calculating the VHR spectra, we use the mean values of the necessary parameters (seismic moment and stress parameter), which are determined from Eqs. (6) and (7). The ratios S_{AS}/S_{VHR} (let us called them as average soil amplification curves),

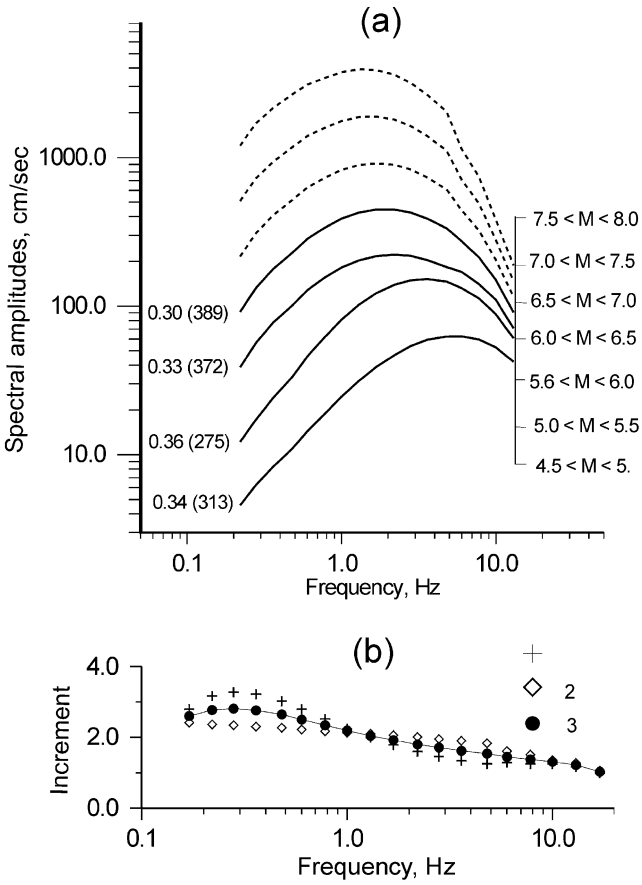

Fig. 2. Average soil spectral model for various intervals of magnitude M. (a) Empirical spectra (solid lines) calculated for reference distance $R = 1$ km. Numbers near the curves denote standard deviation and number of the used records (in parenthesis). Dashed lines show the spectra, which were estimated using the coefficients β_M (see text). (b) Frequency dependence of the coefficients β_M (logarithmic increment of spectral amplitudes) calculated using different intervals of magnitude (1 – $5.5 < M < 6.0$ versus $5.0 < M < 5.5$; 2 – $6.0 < M < 6.5$ versus $5.5 < M < 6.0$; 3—averaged values).

which were calculated for different magnitudes, are shown in Fig. 3(b). The generalised spectral amplification curves for so-called 'generic rock' and 'generic soil', which were proposed for California by Boore and Joyner [12] are also shown in the figure for comparison. It is seen that, on the one hand, the average soil amplification curves estimated for various magnitudes are almost the same. Therefore, the VHR spectral model for the Taiwan region, at least for magnitude range $5.0 < M_L < 6.5$, may be considered as reasonable approximation. When combining with the correspondent site amplification function, the model may be used for site-dependent ground-motion estimations [32]. On the other hand, the amplification curves show almost the same amplitudes for a broad frequency range. Indeed, averaging the variety of site conditions from rock to soft soil of different thickness, the curves reflect both the high-frequency response of a shallow layer and low-frequency amplification of thick soft deposits. At the same time, the amplitudes of the broadband amplification lay between those

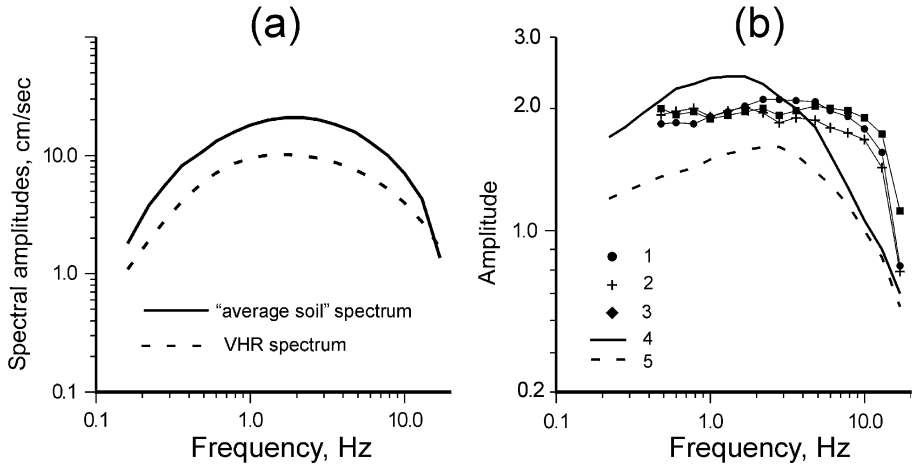

Fig. 3. Relation between VHR and average soil (AS) spectral models. (a) Comparison between the modelled spectra for distance 20 km (VHR model—$M_L = 6.3$; AS model—magnitude range $6.0 < M_L < 6.5$). (b) Comparison of site amplification functions (S_{AS}/S_{VHR}). The curves for the Taiwan region (lines with symbols) were calculated as the ratios between the average soil spectra and VHR spectra, which were estimated for the correspondent magnitudes (1– $6.0 < M_L < 6.5$; 2– $5.5 < M_L < 6.0$; 3– $5.0 < M_L < 5.5$). 4 and 5—the amplification functions for California [12], generic soil and generic rock, correspondingly.

estimated for relatively soft generic soil and rigid generic rock sites [12]. Thus, the ratios S_{AS}/S_{VHR} could be, actually, considered as the regional average soil amplification.

3. Comparison of empirical and modelled data. The Chi-Chi earthquake mainshock

The locations of free field, three-component, accelerograph stations recordings of which are used in this study is shown in Fig. 4. The parameters of source are taken as follows [21,40]: length, 80 km; width, 40 km; strike, 3°; dipping angle, 30° to the East. Fig. 5 shows examples of ground-motion acceleration records obtained at different locations. It is necessary to note that the analyses of the PGA data showed that, on the one hand, the average horizontal PGAs from the earthquake recorded at distances less than 20 km are about 30% below the median PGA based on commonly used attenuation in California [15,37,38]. The comparative analysis of the recordings from small and moderate earthquakes ($5.0 \le M_L \le 6.5$) in the Taiwan region and the Caucasian seismic zones had been performed in Ref. [29]. It had been shown that, in general, the rock-site ground motions in this region are characterised by the lower spectral amplitudes and PGAs for the same magnitude and distance than those in the Caucasus region.

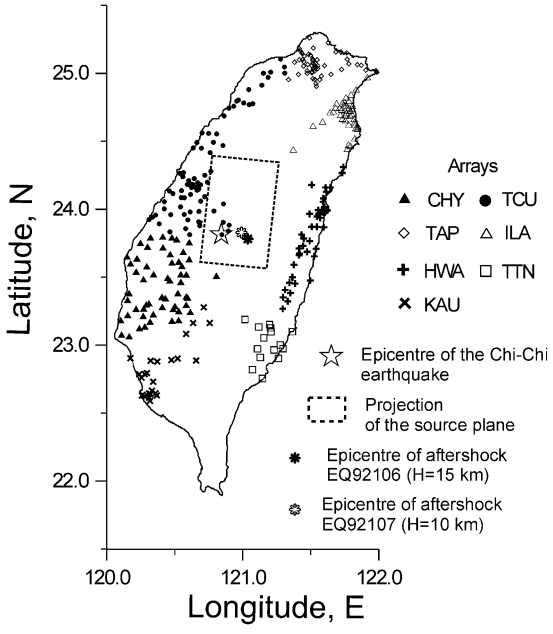

Fig. 4. Location of the free-field digital accelerograph stations, recordings of which were used in this study.

To verify the ability of the average soil spectral model (Fig. 2) to predict the spectral content of ground motion, we compared observed and predicted Fourier amplitude spectra. For this purpose, the obtained records were divided into several groups, by means of distance (the distance increment of 10 km and the intervals containing less than five records were not considered) and location of the stations (the HWA array, eastern direction from the earthquake source; the KAU and TTN arrays, southern direction; the TCU, TAP and ILA arrays, northern direction). The source-site distance is determined as the shortest distance between the source plane and the station. The effects of extended earthquake source [24], which could be observed for the stations TCU and CHY located near the source plane, should be eliminated at the considered distances. We also do not use recordings obtained by the stations that are located to the Northwest, West, and

Fig. 5. Examples of acceleration recordings and spectra obtained during the Chi-Chi earthquake mainshock.

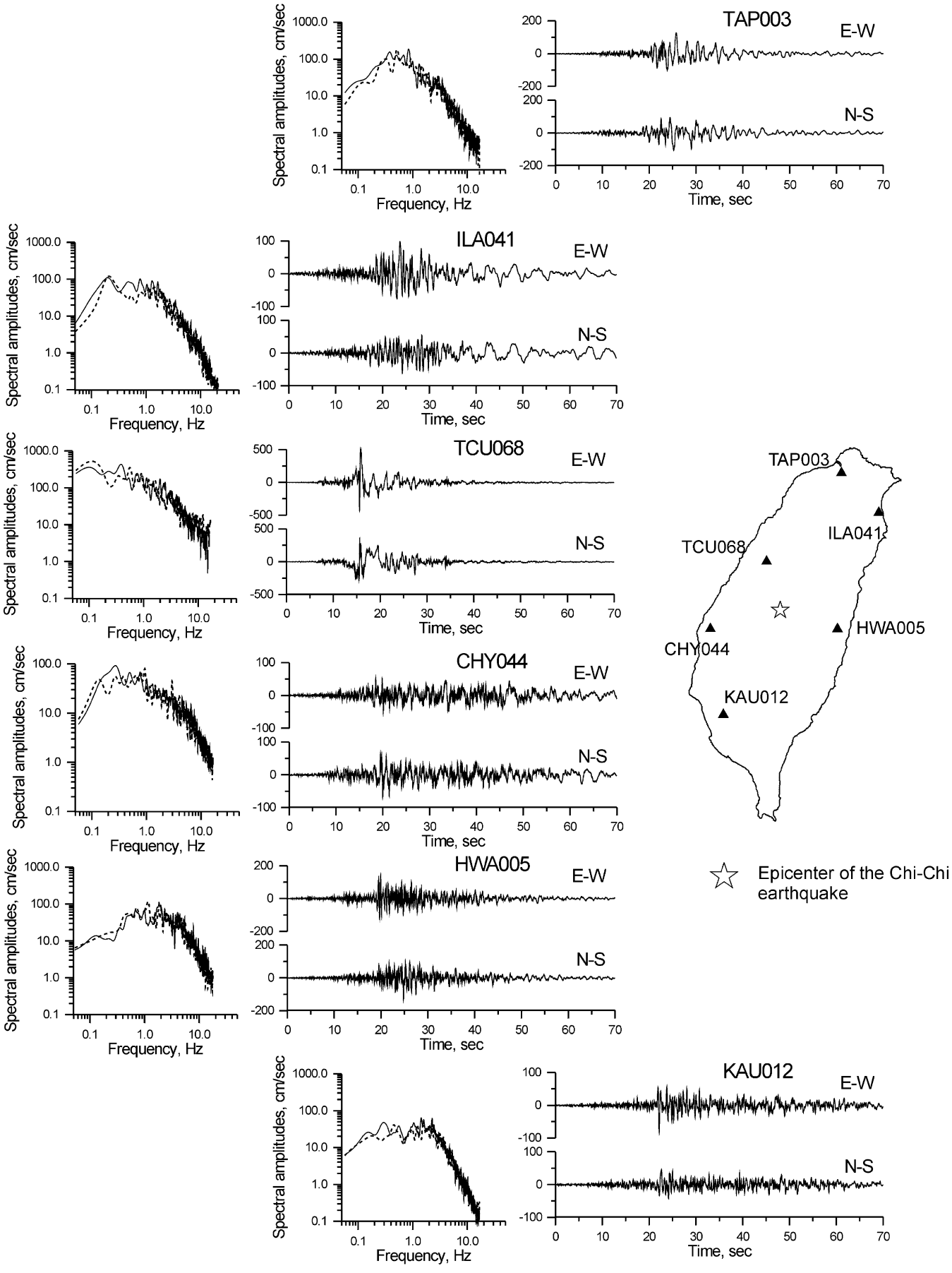
TAP003
E-W
N-S
Spectral amplitudes, cm/sec
Frequency, Hz
Time, sec
ILA041
TCU068
CHY044
HWA005
KAU012
TAP003
ILA041
TCU068
HWA005
CHY044
KAU012
Epicenter of the Chi-Chi earthquake

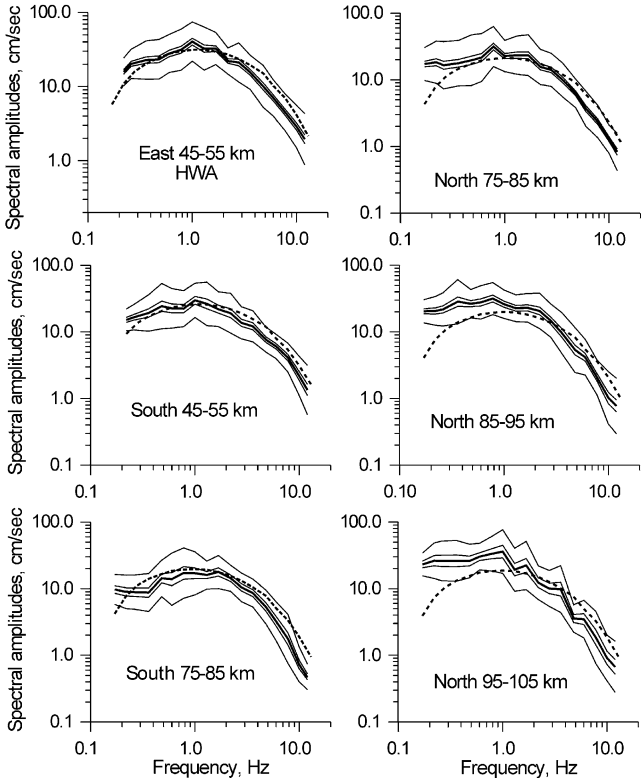

Fig. 6. The Chi-Chi earthquake mainshock. Comparison between observed Fourier amplitude spectra of ground acceleration (solid lines; thick line—average values; thin lines—mean ± 1 std error of means and ± 1 std deviation limits) and simulated, using average soil model (dashed lines), spectra, $Q(f) = 125f^{0.8}$.

Southwest from the epicentre in deep alluvium plain area (the Western Coastal plain). The long-period waveforms that include significant surface waves appear to be the common ground-motion characteristics in the area [16,17]. On the other hand, the stations that are characterised by 'unusual' types of the site response, such as influence of the alluvium-filled valley [23] (several stations of ILA array, see also Fig. 5), are not considered.

Fig. 6 shows the comparison between simulated and observed Fourier amplitude spectra of ground acceleration for the Chi-Chi earthquake mainshock. The average soil spectral model for magnitude interval $7.0 < M_L < 7.5$ and attenuation relation $Q = 125f^{0.8}$ were used, and the modelled spectra were calculated for the centre of corresponding distance intervals. For the eastern and southern directions from the source and intermediate distances (less than 50–60 km), the modelled spectra fit quite well the observed spectra for frequencies less than 3–4 Hz. In high-frequency range, the observed spectra exhibit the lower amplitudes than the modelled ones, and the difference increase with increasing of distance. For northern stations we can see the similar picture in high-frequency range and, for low-frequency band ($f < 1.5$ Hz), observed spectra reveal the larger amplitudes than modelled spectra. On the one hand, the differences between the observed and predicted spectra in low-frequency range are caused by the peculiarities of rupture process of the mainshock source (northward propagation). Furumura et al. [16] on the basis of numerical 2D and 3D simulation concluded that strong diving S-waves, produced by the large shallow asperity of the Chi-Chi earthquake and the large velocity gradient in the crust rigid bedrock, enhance the ground motion to the North from the source at the distances around 80 and 120 km at frequency range less than 1 Hz. On the other hand, the peculiarities of seismic waves propagation from very shallow (depth less than 10 km) earthquakes may be considered as a reason of the difference between observed and modelled spectra in high-frequency range. A study of the strong aftershocks is necessary to verify this suggestion.

4. The Chi-Chi earthquake aftershocks

The aftershocks sequence includes several events of magnitudes $M_L > 6.5$. In this study we used the strong ground-motion data for two aftershocks parameters of which (and the number of used records) are listed in Table 1. In this case the estimation of ground-motion spectra is also based on M_L values and distance from the nearest point of the earthquake source. The sources of the aftershocks were modelled as planes: length, 50 km; width, 30 km. The other parameters of the sources are taken to be similar with the main shock parameters: strike, 3°, and dipping angle, 30° to the East. The centres of the source planes coincide with the reported hypocentres.

Let us consider the data obtained during the aftershock EQ92106. The comparison between modelled (average soil) and observed Fourier amplitude spectra of ground acceleration, which were divided into groups only by means of distance (35–45, 45–55 km, etc.) shows that the modelled and observed spectra reveal a good agreement (Fig. 7(a) and (b)). The average soil spectral model for magnitude interval

Table 1
Parameters of the Chi-Chi earthquake aftershocks, recordings of which are used in this study

Earthquake code	Date and time (UT)	Latitude, N	Longitude, E	Depth, (km)	$M_L(M_W)$	Number of records
EQ92106	1999/09/22, 00:14:40	23°49.58′	121°02.80′	15.6	6.8 (6.4)	360
EQ92107	1999/09/25, 23:52:49	23°51.56′	121°00.35′	9.9	6.8 (6.5)	350

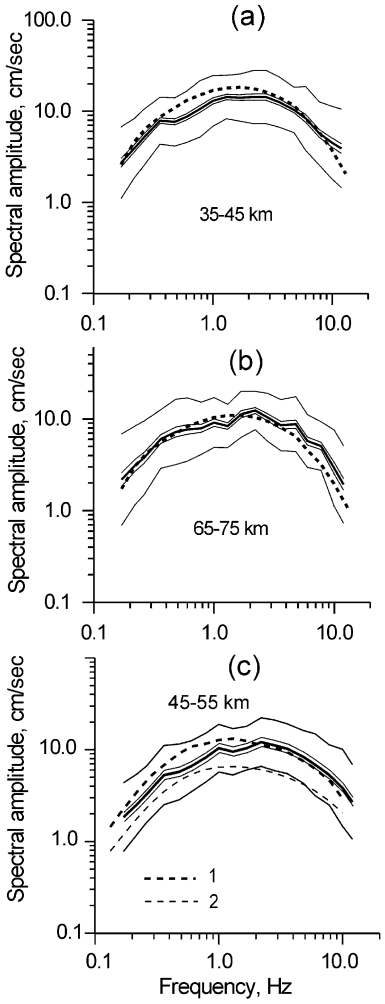

Fig. 7. The aftershock EQ92106. Comparison between observed Fourier amplitude spectra of ground acceleration (solid lines; thick line—average values; thin lines—mean ±1 std error of means and ±1 std deviation limits), and simulated spectra(dashed lines). (a, b) The modelled spectra were obtained using average soil model; (c) the modelled spectra were obtained using VHR model (2) and the VHR model with average soil amplification function (1). Modelled spectra are calculated for the centres of the distance intervals.

$6.5 < M_L < 7.0$ and attenuation relation $Q = 125f^{0.8}$ were used.

Fig. 3(b) shows the average soil spectral amplifications (linear behaviour of soil), which were determined on the basis of the data from earthquakes of $5.0 < M_L < 6.5$. The amplification functions could be used together with VHR spectral model. Therefore, comparison of these models with the observed data could allow us to check the applicability of the models, as well as the used regional relationships between magnitude, seismic moment and stress parameter (Eqs. (6) and (7)) in the case of larger earthquakes. For this purpose, we calculated average soil spectrum at distance 50 km for an earthquake of $M_L = 6.8$ on the basis of VHR model and the average soil amplification function (averaged from three curves, see Fig. 3(b)). The correspondent seismic moment and stress parameter are as follows: $M_0 = 1.8 \times 10^{25}$ dyn cm; $\Delta\sigma = 250$ bars. Fig. 7(c) shows that there is a good agreement between observed (interval 45–55 km) and modelled (VHR model + amplification function) spectra.

Preliminary analysis of the records for the aftershock EQ10297, which occurred at depth 10 km, showed that the high-frequency amplitudes of the observed spectra are characterised by more rapid decrease with distance than those predicted by the model. Therefore, we revised the Q-model using the approach suggested in our previous paper [30]. When considering records from a single earthquake, besides source-dependent variations or peculiarities of the rupture process, the difference between spectral amplitudes at a given frequency is caused by distance-dependent attenuation and site-dependent amplification factors. When partially removing spectral amplitude and shape modification multiplying by $R\exp[\pi fR/Q(f)V_S]$ (i.e. recalculating to reference distance), the scatter of spectral amplitudes, ideally, is determined only by source- and site-dependent factors. Let us suppose that site amplification for the same ground condition does not depend on shaking intensity. Therefore, the proper attenuation model should provide minimum dispersion of the spectral amplitudes $|A|$ for all considered frequencies at reference distance. Thus, it is necessary to analyse values $D_A = (\sum D_f)/N_f$ obtained for different attenuation models. Here D_f is the dispersion of $\log_{10}|A|$ values at frequency f; D_A is the arithmetic average of the D_f values; N is the number of used frequencies. However, the requirement of minimum arithmetic average D_A is not sufficient. Actually, the D_A value does not consider variations of the dispersions at different frequencies, and the optimal attenuation model requires for uniform dispersion of $\log_{10}|A|$ over the entire frequency range. To consider this requirement, it is necessary also to analyse values of the ratio $D_{GA} = D_G/D_A$, where $D_G = (D_1 \times D_2 \times \cdots \times D_N)^{1/N}$ is the geometric average of the values D_f at frequency f_i. The ratio D_{GA} approaches unity under a condition of approximately equal dispersion values at considered frequencies.

The distributions of D_A and D_{GA} values were analysed for various attenuation models ($Q = Q_0 f^n$), and it has been found that in this case the optimal model are characterised by values of $Q_0 = 70–90$ and $n = 0.7–0.9$. The standard deviation of reference-distance spectral amplitudes does not exceed 0.3 log unit. It is interesting to compare the reference-distance spectrum calculated for the aftershock ($M_L = 6.8$) using $Q = 80f^{0.8}$ and the generalised average soil spectra estimated for magnitude range $6.5 < M_L < 7.0$ (Fig. 2(a)) on the basis of data obtained from earthquakes of smaller magnitudes. It is seen (Fig. 8) that the comparison reveals a very good agreement at frequencies more than 1 Hz, and the generalised average soil model shows the smaller amplitudes in low-frequency range. On the one hand, the comparison suggests that the established generalised spectral models could provide a reliable estimation of high-frequency ground-motion parameters for the case of

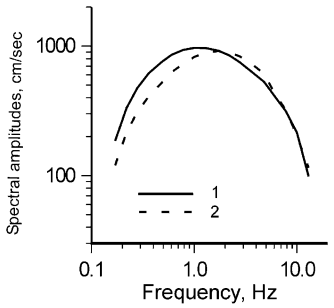

Fig. 8. Mean empirical spectra at the reference distance $R = 1$ km. (1) Spectra which were calculated using records from aftershock EQ92107 ($M_L = 6.8$, depth 10 km, $Q = 80f^{0.8}$). (2) Empirical average soil spectra (magnitude range $6.5 < M_L < 7.0$, see also Fig. 2(a)).

the large event. On the other hand, it is possible to suppose that the large shallow earthquakes in the Taiwan region are characterised by the largest spectral amplitudes at low frequencies (shallow earthquake effect, see also Ref. [33]) than those predicted by the generalised model. It has been found that the values of β_M coefficients for the case of shallow earthquakes should be increased for frequency

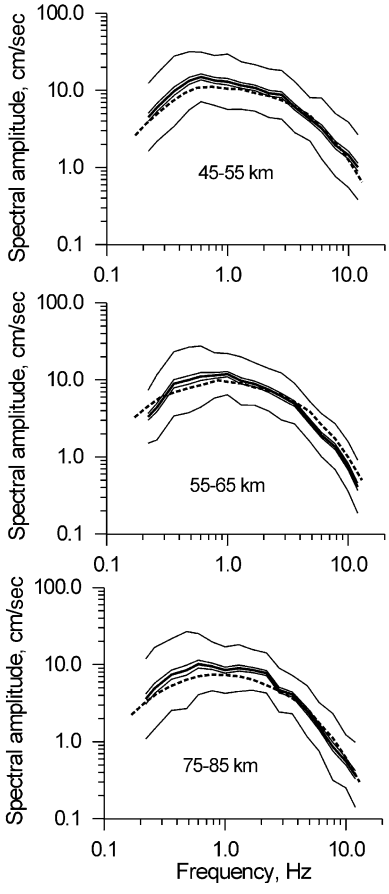

Fig. 9. The aftershock EQ92107. Comparison between observed Fourier amplitude spectra of ground acceleration (solid lines; thick line—average values; thin lines—mean ± 1 std error of means and ±1 std deviation limits), and simulated spectra (dashed lines, average soil model) corrected for the shallow earthquake effect, $Q = 80f^{0.8}$. Modelled spectra are calculated for the centres of the distance intervals.

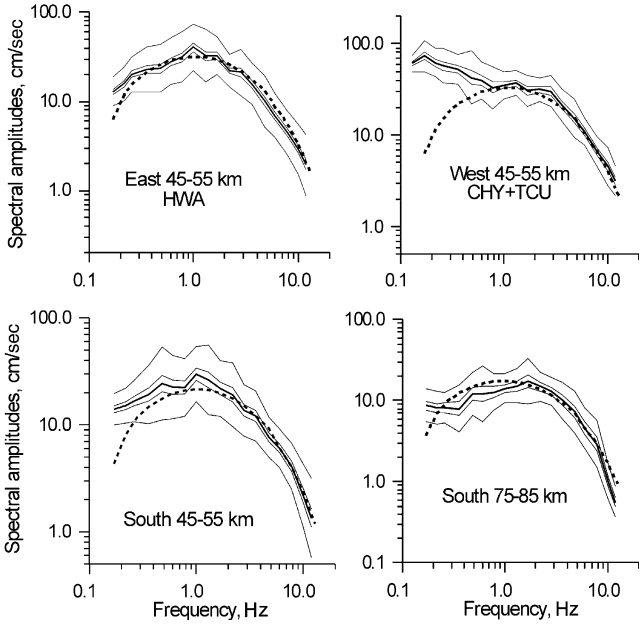

Fig. 10. The Chi-Chi earthquake mainshock. Comparison between observed Fourier amplitude spectra of ground acceleration (solid lines; thick line—average values; thin lines—mean ± 1 std error of means and ±1 std deviation limits) and the simulated spectra (dashed lines, average soil model) corrected for the shallow earthquake effect, $Q = 80f^{0.8}$. Modelled spectra are calculated for the centres of the distance intervals.

range 0.2–1.0 Hz, as compared with those evaluated for the deeper ($H > 10$–15 km) events. By other words, when compiling the model for the shallow earthquakes, the standard β_M coefficients (Fig. 2(b)) should be multiplied by a factor of 1.5 for frequencies 0.2–0.3 Hz, and the factor of multiplication gradually decreases (bearing in mind the logarithmic scale of frequency) to unity for frequencies 1.0–2.0 Hz. However, the suggested 'shallow earthquake' phenomenon should be verified using the data of other earthquakes occurred in the region.

The comparison between modelled, using revised shallow-earthquake average soil spectral model for magnitudes $6.5 < M_L < 7.0$ (Fig. 8), and observed Fourier amplitude spectra of ground acceleration from aftershock EQ92107, which were divided into groups by means of distance, shows that the modelled and observed spectra in general fit each other (Fig. 9).

The average soil spectral model for magnitude interval $7.0 < M_L < 7.5$ combined with revised attenuation model $Q(f) = 80f^{0.8}$ was also checked for the Chi-Chi earthquake mainshock. Fig. 10 shows the examples of comparison between simulated and observed Fourier amplitude spectra of ground acceleration for the mainshock. The modelled spectra calculated for correspondent distances fit the mean amplitudes of observed spectra at frequencies 0.2–12 Hz both for eastern (HWA array) and southern directions. We also use for comparison records from stations of CHY and TCU arrays located to the West from the Chi-Chi earthquake source. These stations are located in deep alluvium plain area, so-called Western Coastal plain.

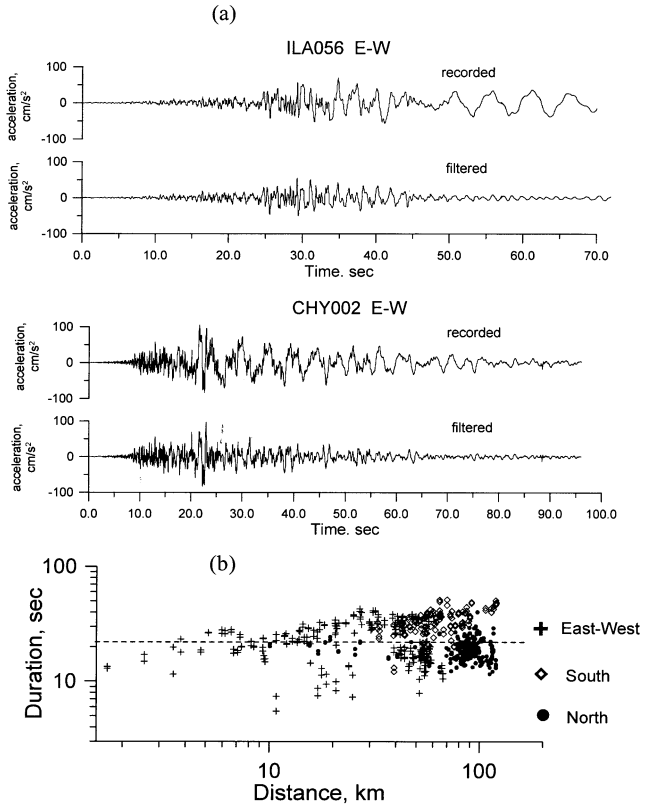

Fig. 11. Evaluation of significant duration of ground acceleration during the Chi-Chi earthquake (mainshock). (a) Examples of recorded and filtered (high-pass above 0.4 Hz) accelerograms. (b) Distribution of significant duration versus distance, dashed line shows average value − 22 s.

The long-period waveforms that include significant surface waves appear to be the common ground-motion characteristics in the area [16,17]. In this case the observed spectra, showing a good agreement with modelled spectra at frequencies more than 0.7–0.8 Hz, exhibit sufficiently larger amplitudes at frequencies less than 0.6–0.7 Hz. Obviously, the difference is caused by surface waves generated by the mainshock in this area.

5. Discussion

The suitability of any spectral model and attenuation relation proposed for engineering purposes should be evaluated by the capability of the models to predict peak ground amplitudes (PGA) and response spectra versus earthquake and distance. In the considered case, the stochastic simulation technique introduced by Boore [10] was used. One of the most important parameters of the stochastic predictions is the duration model, because it is assumed that most (90%) of the spectral energy given by Eq. (1) is spread over a duration $\tau_{0.9}$ (so-called 'significant duration') of the accelerogram. It has been found in our previous study [30,31] that the regional relationship between ground-motion duration ($\tau_{0.9}$) and magnitude proposed by Wen and Yeh [39] in the following form

$$\tau_{0.9} = 0.43 \exp(0.504 M_L) \pm 2.749 \quad (8)$$

give a better fit to empirical data. A value that equals to 17(±2.75) s should be used for earthquake of magnitude M_L 7.3 according to the relationship. We made an attempt for preliminary evaluation of the ground-motion duration using the registered accelerograms. The duration is defined as the interval between the times at which 5 and 95% of the Arias intensity integral is attained [34]. We use the generalised VHR and average soil spectral models in our comparison therefore it is necessary to estimate the duration excluding such extreme effects as a propagation of long-period surface waves along the alluvial basins. The examples of such phenomenon could be clearly seen for the central part of the Ilan area (station ILA041, Fig. 5). Thus, the high-pass filtering procedure has been applied to every accelerogram (see Fig. 11(a)), and we calculated the duration for the motion in the frequency range above 0.4 Hz. Fig. 11(a) shows examples of the filtering. In this case the influence of the 'location-dependent' long-period waves, which were observed in the near-source ground acceleration (for example, station TCU068, Fig. 5) and caused by the peculiarities of the source rupture process or by influence of geological condition, was also eliminated.

The analysis of distribution of duration versus the distance to the Chi-Chi earthquake source revealed no dependence on the distance (Fig. 11(b)). Table 2 lists the statistical parameters of ground-motion duration (average value and standard deviation) determined for the whole data set, and for the stations located toward various directions from the source plane. The influence of rupture peculiarities or (and) azimuthal variation of attenuation could be clearly seen. The effective duration of ground-motion acceleration toward the South from the source is, in general, 1.4–1.5 times higher than that toward the North. At the same time, the duration along the latitudinal directions may be considered as 'average' one, and the average value of 22 s is close to that predicted by the Wen and Yeh's relationship (17 ± 2.75 s). On the one hand, these features of effective duration may be described by peculiarities of the slip distribution along the fault plane [19,21,40]. The area of largest slip dislocation is located about 30–50 km north of

Table 2
Results of the effective duration determination for the Chi-Chi earthquake mainshock

Statistical parameters of the effective duration	The whole data set	Northern direction	Southern direction	E–W direction
Average value (s)	22.2	18.2	30.1	22.0
Standard deviation of $\log_{10} \tau_{0.9}$	0.16	0.09	0.17	0.15

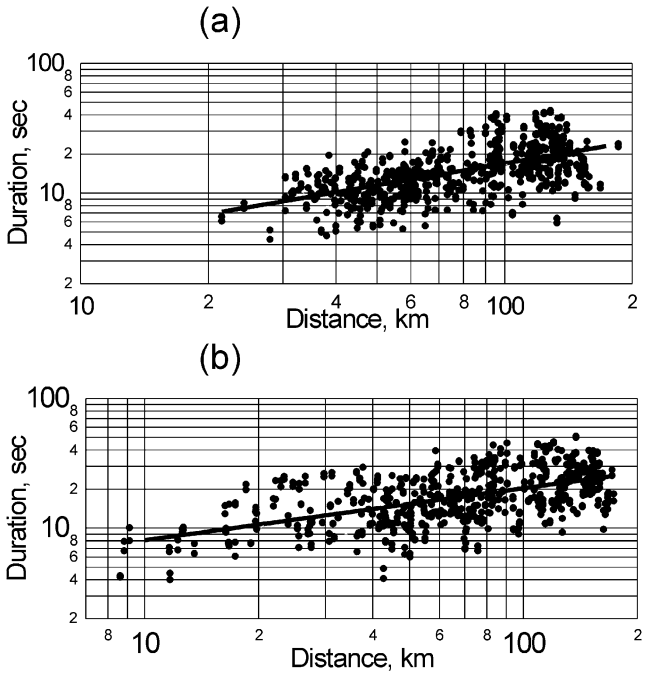

Fig. 12. Distribution of significant duration versus distance; (a) aftershock EQ92106; (b) aftershock EQ92107.

the hypocentre. Therefore, the influence of this large subsource and the south-north propagation of the rupture front may cause the shorter duration of strong ground motion toward the North from the earthquake source.

The distribution of significant duration versus distance for the considered aftershocks reveals an increase of duration with increasing of the distance (Fig. 12). The dependence may be described as $\tau_{0.9} = 1.29R^{0.56}$ or $\log_{10}\tau_{0.9} = (0.11 \pm 0.054) + (0.56 \pm 0.028)\log_{10} R$ for the aftershock EQ92106, and $\tau_{0.9} = 3.64R^{0.37}$ or $\log_{10}\tau_{0.9} = (0.5 \pm 0.043) + (0.41 \pm 0.023)\log_{10} R$ for the aftershock EQ92107. Therefore, when applying the spectral models for the aftershocks, the ground-motion parameters were determined using distance-dependent effective duration.

Fig. 13 shows the comparison between empirical PGA (horizontal components) and those calculated using the VHR and the average soil spectral models. A set of 40 synthetic acceleration time functions was generated, and the resulting PGA is estimated as an average value. The distribution of the PGA values is shown versus the shortest distance to the rupture (fault plane). When calculating theoretical PGAs, the minimum site-rupture distance to be used in Eqs. (2) and (4) was accepted as $R = 10$ km, because, as it has been revealed from empirical attenuation models, the ground-motion parameters insignificantly vary with distance near earthquake source (the so-called 'near-field zone'). The dimension of this zone (the shortest distance to the source plane) for $M = 7$ earthquake is approximately equal to 10 km [14]. When applying VHR spectral model, the necessary earthquake parameters (seismic moment and stress parameter) were evaluated

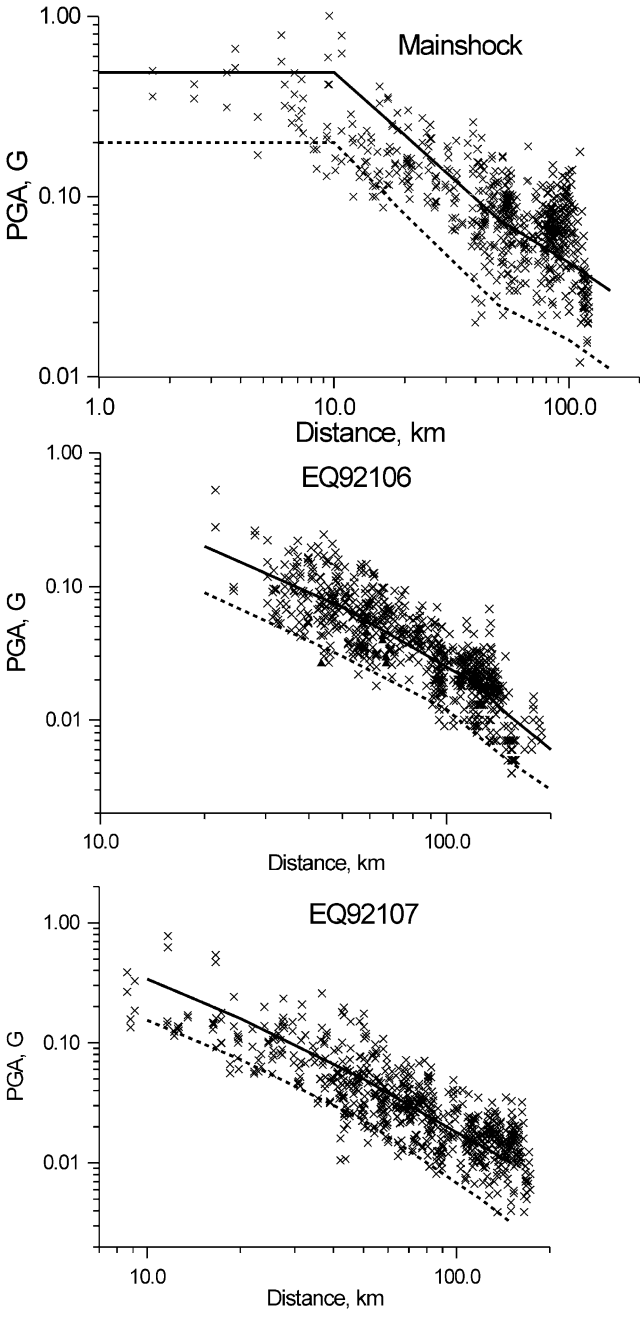

Fig. 13. Distribution of the observed PGA values (horizontal components, symbols) and the predicted amplitudes for the Chi-Chi earthquake mainshock and considered aftershocks. The lines show PGA values calculated using different spectral models: dashed line—VHR spectra; 2 solid line—average soil spectra.

from regional relationships 6 and 7. The parameters were taken as follows: the mainshock ($M_L = 7.3$, $M_0 = 5.2 \times 10^{25}$ dyn cm, $\Delta\sigma = 320$ bars); the aftershocks ($M_L = 6.8$, $M_0 = 1.8 \times 10^{25}$ dyn cm, $\Delta\sigma = 250$ bars). It is necessary to note, that we do not consider the values reported for the earthquakes. Our goal is to estimate whether is it possible to use the recently developed spectral model, which is based on averaged regional relationships, for the case of future large event. The Chi-Chi earthquake and

Table 3
Parameters of residuals distribution for the Chi-Chi earthquake and aftershocks (PGA data)

Earthquake	Number of values	Average value	Standard deviation
The Chi-Chi mainshock	652	−0.027	0.22
EQ92106	743	0.015	0.19
EQ92107	706	−0.05	0.30

aftershocks are considered as the examples of such events. However it is necessary to note that the parameters of largest asperity (subsource) of the Chi-Chi source determined in Ref. [19] are approximately the same: $M_0 = 11 \times 10^{25}$ dyn cm, $\Delta\sigma = 200$ bars.

It is seen that the peak amplitudes, which were calculated using VHR model, are less than the observed amplitudes and provide a kind of 'lower limit' estimation. The average soil model, in general, provides a satisfactory prediction for the case of the Chi-Chi earthquake (constant duration 20 s) and for the aftershocks (distance-dependent duration). The statistical parameters for the residuals between modelled PGAs and observed values are listed in Table 3. The residuals are defined as the log (base 10) of the ratio of the observed ground-motion amplitude to the predicted value. The empirical and modelled 5% damped response spectra are compared in Fig. 14. When calculating spectra for the mainshock and the aftershock EQ92107, we used the average soil spectral model revised for the shallow-earthquake effect and $Q = 80f^{0.8}$, and the standard average soil spectral model (Fig. 2(a)) and $Q = 125f^{0.8}$ were used for the aftershock EQ92106. It is seen that the modelled response spectra show a good agreement with the averaged empirical spectra in the whole considered frequency range.

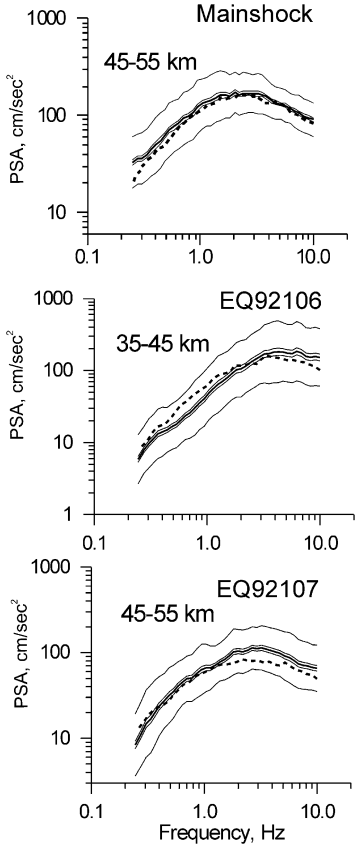

Fig. 14. Comparison between the observed 5% damped response spectra (solid lines; thick line—average values; thin lines—mean ± 1 std error of means and ± 1 std deviation limits), and simulated, using average soil spectral model, spectra (dashed lines).

6. Conclusion

The comparison of the ground-motion data collected during the $M_L = 7.3$ Chi-Chi earthquake and large aftershocks ($M_L = 6.8$) makes it possible to conclude that the regional empirical models for Fourier amplitude spectra of ground acceleration, which were developed recently using the database from small and moderate earthquakes ($4.5 < M_L < 6.5$), allow satisfactory prediction of peak ground acceleration and response spectra for large earthquakes. When predicting ground-motion spectra on the basis of spectral model for hypothetical VHR site, the recently proposed regional relationships between seismic moment (M_0) and magnitude (M_L), and between $\Delta\sigma$ and M_0 are used. It has been found that for the case of the Chi-Chi earthquake mainshock ($M_L = 7.3$) these relationships produce the $\Delta\sigma$ and M_0 values that are similar to the correspondent parameters of the source largest asperity (subsource): $M_0 = 5.2 \times 10^{25}$ dyn cm, $\Delta\sigma = 320$ bars (Eqs. (6) and (7) for $M_L = 7.3$); $M_0 = 11 \times 10^{25}$ dyn cm, $\Delta\sigma = 200$ bars for the largest asperity [19]. Therefore, it is possible to conclude that the use of regional relationships, which are based on local magnitude M_L, allow to predict high-frequency acceleration parameters for the earthquakes in the Taiwan area.

At the same time, the study of the large collection of acceleration records (more 1200 accelerograms) revealed several peculiarities of strong ground-motion excitation and propagation during large shallow earthquakes in the central Taiwan area. Some of them may be described by the characteristics of slip distribution along the fault plane. These peculiarities include the evidence of the greater duration of vibration for the stations located to the southern direction from the Chi-Chi earthquake source, as compared with the stations located to the North. The other should be considered as intrinsic characteristics of shallow earthquakes of the region: the larger low-frequency

spectral amplitudes and more rapid attenuation of spectral energy than those for the deeper (depth more 10–15 km) events. These features could be explained by the properties of the Earth's crust in the region. For example, the ground-motion spectra from earthquakes, which occurred in rigid and consolidated medium (eastern North America, or Central Asia), are characterised by predominance of high-frequency amplitudes [4,11,14]. The phenomenon could be described by the presence of strong asperities or barriers [1] along the fault plane. The stronger asperities—the higher amplitudes of the high-frequency part of the spectra. On the other hand, the attenuation of spectral energy is lesser in harder rocks and tectonically stable regions. Therefore, the ratio between low- and high-frequency spectral amplitudes of ground motion should increase with decreasing of the earthquake depth and weakening the rock rigidity—smooth rupture produces long-period waves. It is necessary to note, that relatively high-spectral amplitudes in the low-frequency domain were observed both at close distances from the Chi-Chi earthquake source and aftershocks, and in far-field zone.

Acknowledgments

The study was carried out in National Center for Research on Earthquake Engineering and was supported by the National Science Council of the Republic of China under grant NSC89-2811-E-319-005.

References

[1] Aki K. Asperities, barriers, characteristic earthquakes and strong motion prediction. J Geophys Res 1979;89:5867–72.
[2] Anderson J, Hough S. A model for the shape of the Fourier amplitude spectrum of acceleration at high frequencies. Bull Seism Soc Am 1984;74:1969–93.
[3] Atkinson GM, Mereu RF. The shape of ground motion attenuation curves in southeastern Canada. Bull Seism Soc Am 1992;(82): 2014–31.
[4] Atkinson GM. Earthquake source spectra in Eastern North America. Bull Seism Soc Am 1993;(83):1778–98.
[5] Atkinson GM, Boore DM. Ground-motion relations for eastern North America. Bull Seism Soc Am 1995;(85):17–30.
[6] Atkinson GM, Silva W. An empirical study of earthquake source spectra for California earthquakes. Bull Seism Soc Am 1997;(87): 97–113.
[7] Atkinson GM, Silva W. Stochastic modelling of California ground motions. Bull Seism Soc Am 2000;(90):255–74.
[8] Beresnev IA, Atkinson GM. Stochastic finite-fault modelling of ground motions from the 1994 Northridge, California, earthquake. I. Validation on rock sites. Bull Seism Soc Am 1998;(88):1392–401.
[9] Boatwright J, Choy G. Acceleration source spectra anticipated for large earthquakes in northeastern North America. Bull Seism Soc Am 1992;(82):660–80.
[10] Boore DM. Stochastic simulation of high frequency ground motion based on seismological model of the radiated spectra. Bull Seism Soc Am 1983;73:1865–94.
[11] Boore DM, Atkinson GM. Stochastic prediction of ground motion and spectral response parameters at rock sites in eastern North America. Bull Seism Soc Am 1987;(77):440–67.
[12] Boore DM, Joyner WB. Site amplification for generic rock sites. Bull Seism Soc Am 1997;87:327–41.
[13] Brune JN. Tectonic stress and the spectra of seismic shear waves from earthquakes. J Geophys Res 1979;(75):4997–5009.
[14] Chernov YuK. Strong ground motion and quantitative assessment of seismic hazard. Tashkent: Fan Publishing House; 1989. in Russian.
[15] Earthquake Engineering Research Institute. The Chi-Chi Taiwan earthquake of September 21, 1999. EERI Special Earthquake Report 1999.
[16] Furumura T, Koketsu K, Wen KL, Furumura M. Numerical simulation of strong ground motion during the Chi-Chi, Taiwan, earthquake. Proceedings of the International Workshop on Annual Commemoration of Chi-Chi Earthquake, vol. 1, September 18–20, 2000, NCREE, Taipei; 2000. p. 222–32.
[17] Huang CT, Chen SS. Near-field characteristics and engineering implications of the 1999 Chi-Chi earthquake. Earthquake Engng Engng Seismol 2000;(2):23–41.
[18] Hwang LG, Kanamori H. Teleseismic and strong-motion source spectra from two earthquakes in eastern Taiwan. Bull Seism Soc Am 1989;(79):935–44.
[19] Irikura K, Kamae K, Dalguer LA. Source model for simulating ground motion during the 1999 Chi-Chi earthquake. Proceedings of International Workshop on Annual Commemoration of Chi-Chi Earthquake, vol. 1, September 18–20, 2000, NCREE, Taipei; 2000. p. 1–12.
[20] Lam N, Wilson J, Hutchinson G. Generation of synthetic earthquake accelerograms using seismological modelling: a review. J Earthquake Engng 2000;(4):321–54.
[21] Lee SJ, Ma KF. Rupture process of the 1999 Chi-Chi, Taiwan, earthquake from the inversion of teleseismic data. Terrestial, Atmospheric Ocean Sci 2000;(11):591–608.
[22] Li C, Chiu HC. A simple method to estimate the seismic moment from seismograms. Proc Geol Soc China 1989;32:197–207.
[23] Liu LF, Wen KL. The site response of Lanyang basin on the Chi-Chi earthquake sequence. Proceedings of International Workshop on Annual Commemoration of Chi-Chi earthquake, vol. 1, Taipei, Taiwan; 2000. p. 294–304.
[24] Loh CH, Lee ZK, Wu TC, Peng SY. Ground motion characteristics of the Chi-Chi earthquake of 21 September 1999. Earthquake Engng Struct Dyn 2000;(29):867–97.
[25] Rovelli A, Bonamassa O, Cocco M, Di Bina M, Mazza Z. Scaling laws and spectral parameters of the ground motion in active extensional areas in Italy. Bull Seism Soc Am 1988;78:530–60.
[26] Shin TC, Kuo KW, Lee WHK, Teng TL, Tsai YB. A Preliminary report on the 1999 Chi-Chi (Taiwan) Earthquake. Seismol Res Lett 2000;(71):24–30.
[27] Sokolov V. Spectral parameters of the ground motions in Caucasian seismogenic zones. Bull Seism Soc Am 1998;(88):1438–44.
[28] Sokolov V. Ground acceleration spectra from Caucasus earthquakes. Izvestiya. Phys Solid Earth 1998;(34):663–75.
[29] Sokolov V. Spectral parameters of ground motion in different regions: comparison of empirical models. Soil Dyn Earthquake Engng 2000; (19):173–81.
[30] Sokolov V, Loh CH, Wen KL. Empirical models for estimating design input ground motions in Taiwan region. Proceedings of International Workshop on Mitigation of Seismic Effects on Transportation Structures, Taipei, Taiwan; July 12–14, 1999. p. 154–63.
[31] Sokolov V, Loh CH, Wen KL. Empirical model for estimating Fourier amplitude spectra of ground acceleration in Taiwan region. Earthquake Engng Struct Dyn 2000;(29):339–57.
[32] Sokolov V, Loh CH, Wen KL. Empirical study of sediment-filled basin response: a case of Taipei city. Earthquake Spectra 2000;(16): 681–707.

[33] Somerville PG. Magnitude scaling of near fault ground motions. Proceedings of International Workshop on Annual Commemoration of Chi-Chi earthquake, vol. 1, Taipei, Taiwan; 2000. p. 59–70.

[34] Trifunac MD, Brady AG. A study of the duration of strong earthquake ground motion. Bull Seismol Soc Am 1975;65: 581–626.

[35] Trifunac MD, Lee VW. Empirical models for scaling Fourier amplitude spectra of ground acceleration in terms of earthquake magnitude, source to station distance, site intensity and recording site conditions. Soil Dyn Earthquake Engng 1989;(8):110–25.

[36] Tsai CCP. Relationships of seismic source scaling in the Taiwan region. Terrestial, Atmospheric Ocean Sci 1997;(8):49–68.

[37] Tsai YB, Huang MW. Strong ground motion characteristics of the Chi-Chi, Taiwan earthquake of September 21, 1999. Earthquake Engng Engng Seismol 2000;2:1–21.

[38] Wang CY, Chang CH, Yen HY. An interpretation of the 1999 Chi-Chi earthquake in Taiwan based on thin-skinned thrust model. Terrestial, Atmospheric Ocean Sci 2000;11:609–30.

[39] Wen KL, Yeh YT. Characteristics of strong motion durations in the SMART1 array area. Terrestial, Atmospheric Ocean Sci 1991;2: 187–201.

[40] Yagi Y, Kikuchi M. Source rupture process of the Chi-Chi, Taiwan earthquake determined by seismic waves and GPS data. Eos Trans AGU 2000;81(22). S21A-05.